Frequency difference mapping at 7 T using two- and three-echo approaches

Samuel Wharton[1] and Richard Bowtell[1]

[1]*Sir Peter Mansfield Magnetic Resonance Centre, School of Physics and Astronomy, University of Nottingham, Nottingham, United Kingdom*

Introduction: The strong anisotropic magnetic susceptibility of the myelin sheath gives rise to significant differences in the average frequencies of the NMR signals arising from the myelin, intra-axonal and extra-axonal compartments in white matter [1]. These frequency differences depend on the nerve fiber orientation with respect to the magnetic field, B_0. As a result of the rapid T_2 relaxation of the myelin water relative to that found in the other compartments [2], these frequency differences produce a non-linear evolution of the WM signal phase, ϕ, as a function of echo time, TE, which is manifested as a change in the effective frequency of signal evolution, $f = \phi/TE$, with TE [1,3]. Frequency difference mapping, in which the difference in the effective frequencies at short and long TE is calculated from phase data generated using simple gradient echo sequences, thus provides a new method of generating high resolution images displaying contrast that is sensitive to WM microstructure and the orientation of nerve fibers with respect to B_0. In order to measure the small frequency change due to the decay of the myelin water signal it is necessary to eliminate the effect of other TE-independent phase offsets, such as those due to sample-induced spatial variation in the phase of the applied RF [4,5], as well as cancelling out the non-local frequency offsets, due for example to poor shimming. This can be accomplished by high-pass filtering the frequency difference map (FDM) formed from phase data generated at two echo times or by subtracting off the phase from a measurement at a third echo time, before calculation of the effective frequency difference [1,3]. The purpose of this work was to use simulations and experiments to investigate the optimum TE values for creating high quality *in vivo* FDM at 7T using two or three echoes and to compare the quality of the resulting frequency difference maps.

Methods: (Simulations) The phase evolution for a myelinated fiber oriented at 60° (the expected average fiber orientation) to B_0 was simulated using the hollow cylinder model described in recent work [1]. In this model, the myelin sheath is represented as a hollow cylinder formed from material of anisotropic magnetic susceptibility, with a radially oriented principal axis, and the signal from the sheath decays faster than the surrounding space to allow for the shorter T_2 of myelin water (set to 10ms in this model versus 36 ms for other compartments [1]). Figure 1A shows a map of the simulated frequency perturbation due to the hollow cylinder model (g-factor= 0.8, fiber volume fraction = 0.5), where the sheath corresponds to the annulus in which there is a strong positive frequency offset. Figure 1B shows the non-linear phase evolution with TE for this model, which was produced by subtracting off a linear fit to the variation of the phase from the sample with TE. As would be expected, the resulting phase peaks at a time that is approximately equal to the T_2 of the myelin water. Assuming that the noise in the phase measurements is proportional to the magnitude signal to noise ratio, we determined the TE values that would yield FDM with the highest SNR in two different acquisition schemes: (i) a two echo acquisition (TE_1, TE_2) where the FDM are created by scaling the phase values by TE and taking the difference - i.e. $\Delta f = \phi_2/TE_2 - \phi_1/TE_1$; (ii) a three echo scheme (TE_1, TE_2, TE_3) where frequency maps are formed by dividing the phase difference between the two echoes by the difference in TE - i.e. $f_{21} = (\phi_2 - \phi_1)/(TE_2 - TE_1)$ and the frequency difference is given by $\Delta f = f_{32} - f_{21}$. Assuming that the shortest accessible TE was 2 ms, the optimum TE values were estimated to be TE_1/TE_2 = 4/25ms for the two echo scheme (blue circles in Fig.1B) and $TE_1/TE_2/TE_3$ = 2/7/23ms for the three echo scheme (red squares in Fig.1B). The calculated SNR for the optimised two echo scheme was 1.5 times higher than the optimised three echo scheme. On the scanner for technical reasons the maximum achievable value of TE_3 was 17 ms which reduced the 3-echo SNR by 11%. **(Data Acquisition)** A healthy male subject (age = 30 years) was scanned at 7T using GE sequences with FOV=224x224x50 mm^3, isotropic resolution=2mm and TR =32ms. For the two echo scheme, a standard 3D spoiled multi-echo GE sequence was used: TE_1/TE_2=4/25ms, FOV=224x224x50 mm^3, NEX = 4, scan time = 6min. For the three echo scheme, we used two dual-echo B_0-mapping sequences to facilitate data processing: TE_1/TE_2=2/7ms for the first scan, TE_2/TE_3=7/17ms for the second, NEX = 2, scan time=2×3min=6min. FDM were then created from the reconstructed phase data from the image data at two or three echo times as described above. It was necessary to unwrap the phase of the two-echo data before creating the FDM, but the three echo data could be handled in complex form and did not require unwrapping.

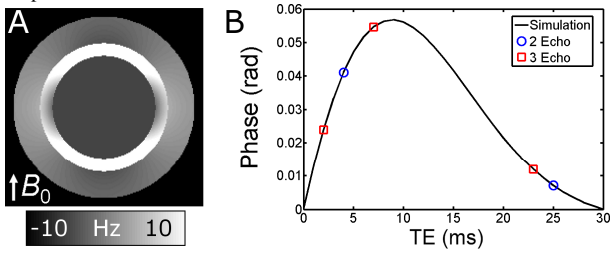

Fig 1 – (A) Frequency perturbation map due to the hollow cylinder model. (B) Simulated local phase evolution.

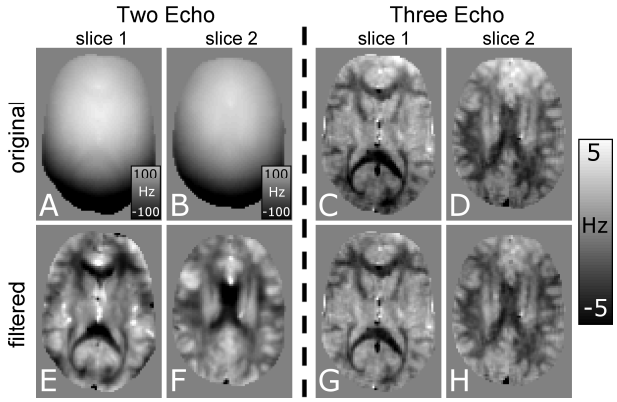

Fig 2 – Axial slices of the FDM reconstructed from the two echo (A,B,E,F) and three echo data (C,D,G,H) before high-pass filtering (A-D) and after filtering (E-H) in a healthy subject.

Results: Figure 2 shows two representative axial slices at the level of the optic radiations (slice 1) and the corpus callosum (slice 2) of the reconstructed FDM data based on the two- and three-echo data. Figure 2A&B show that the raw two-echo FDM is dominated by a large length-scale spatial variation most likely originating from RF transmit phase effects [4]. Through trial and error it was found that the fitting and subtraction of a 6th order, 3D polynomial was necessary to remove this "bias field" and reveal the effects due to WM structures (Fig. 2G&H). In contrast, the three-echo FDM is well behaved before any spatial filtering (Fig. 2C&D), as the underlying frequency maps (f_{21} and f_{32}) are theoretically insensitive to transmit phase effects These data only required the fitting and subtraction of a 1st order, 3D polynomial to remove a small anterior-posterior gradient (0.3 Hz/cm) in the contrast (Fig. 2G&H), most likely arising from small differences in eddy current effects in the underlying frequency maps. The filtered two- and three-echo FDM show strong (negative) contrast in the WM fiber tracts that are perpendicular to B_0, consistent with previous reports [2]. The SNR of the two-echo FDM is higher than the three-echo FDM, in line with the simulations. The filtered two-echo FDM exhibits some small length scale contrast variations in regions close to large blood vessels, particularly in the grey matter, most likely resulting from the effects of the high-pass spatial filtering step. This is in contrast to the spatially consistent GM/WM contrast exhibited in the three-echo FDM.

Discussion: The results of the *in vivo* data acquisition suggest that high-quality FDM exhibiting contrast that is dependent on the local fiber orientation in WM can be created from gradient echo images acquired at two or three echo times at 7T in a time of around six minutes. Frequency difference mapping could thus form a powerful technique for visualising WM microstructure in the human brain. Simulations indicate that the achievable SNR is higher for the two-echo scheme (when the minimum achievable TE is 2ms), but the two-echo approach requires the application of phase unwrapping and more importantly, the fitting and subtraction of a high-order polynomial to eliminate the effect of TE-independent phase terms, most likely arising from RF transmit phase variation. The latter step has some disadvantages for producing uniform contrast sensitivity over images. The three-echo approach requires minimal data processing and so may be readily implemented on the scanner to facilitate future studies.

References: [1] Wharton and Bowtell, 2012, PNAS, doi:10.1073/pnas.1211075109; [2] Mackay et al. MRM. 1994. (31) 673-677; [3] Schweser et al. Proc. ISMRM 2011 # 1428; [4] Schweser et al. Neuroimage. 2010. (54) 2789-2807; [5] van Lier et al. MRM 2012 (67) 552-561.